



---

**Research Paper**

---

**Development of a Technique for Increasing the Directivity of an Antenna Array in the Microwave Range**

**I.J. ISLAMOV<sup>1,a</sup>, A.T. RAHIMOV<sup>1,b</sup>, M.M. JAHANGIROV<sup>1,c</sup>, N.M. SHUKUROV<sup>1,d</sup>,  
R.S. ABDULLAYEV<sup>1,e</sup>**

<sup>1</sup>Department of Radio Engineering and Telecommunication, Azerbaijan Technical University, Baku, Azerbaijan  
<sup>a</sup>icislamov@mail.ru

**Received:** 13.04.2023

**Accepted:** 14.08.2023

---

**Abstract:** The paper proposes and tests an effective method for improving the directivity of diffraction-type leaky-wave antennas based on the implementation of a longitudinal change in the profile of the distribution-radiating system due to the variation of the aiming distance according to a given amplitude distribution. It has been established that changing the aiming distance along the aperture according to a theoretically calculated regularity makes it possible to improve the initial directional properties of the antenna: to reduce the maximum level of side lobes, and also to increase the antenna gain.

**Keywords:** microwave range, antenna array, side lobe level, gain, radiation patterns

---

## 1. Introduction

The innovative way of development of radio engineering systems is closely connected with the development of the short-wave part of the centimeter range, millimeter and submillimeter wave ranges. The most promising at present is the use of these ranges to create ultra-high-speed wireless transport networks for mobile traffic. Such networks are already capable of providing data transfer rates up to 10 Gbit/s based on simple modulation methods without the use of additional coding algorithms [1, 2]. At the same time, the features of the propagation of radio waves in the centimeter and millimeter ranges make it possible to implement a number of widely demanded radio engineering and info communication systems for communication, navigation and control applications. These include microwave radiometric scattering complexes for environmental studies, systems for observing objects in conditions of limited visibility, and active survey radar stations [3-5].

For the efficient operation of radio engineering systems in the microwave and extremely high frequencies bands, it is necessary to equip them with antennas that have a high efficiency and are capable of forming highly directional radiation patterns in space. As such antennas, diffraction-type leaky-wave antennas (DTLWA) can be used, which are a reflective grating, for example, a comb type, covered with a dielectric layer. The main advantages that distinguish diffractive antennas from other types of antennas are the simplicity and reliability of the design, high manufacturability with the possibility of a continuous production principle due to the repeatability of dimensions, small weight and size characteristics and low cost indicators.

The principle of operation of the DTLWA is based on the spatial transformation of a received free wave by a resonant diffraction grating into a surface wave of an open decelerating line [6, 7]. This kind of conversion is characterized by a high directional coefficient, reaching more than 95% for individual optimized antenna samples [4]. The task of providing a low level of lateral radiation and

*How to cite this article*

increasing the efficiency of using the opening surface can be solved by implementing the optimal amplitude distribution of the field in the opening by changing the groove depth in the longitudinal direction and varying the aiming distance - the gap between the flat dielectric waveguide and the comb grating. The possibilities of optimizing the characteristics of the DTLWA due to the depth profiling of a one-dimensional quasi-periodic comb array at a fixed aiming distance are considered in sufficient detail in [8, 9]. The purpose of this work is to develop and test a technique for increasing the directivity of DTLWA by providing a longitudinal variation of the key geometric parameter of the distribution-radiating system - the aiming distance.

## 2. Formulation of the Problem

On Fig. 1 shows in cross-section the model geometry of the distribution-radiating system of DTLWA, including an equidistant (with a period  $d$ ) comb resonant a diffraction grating with a finite number of identical grooves (width  $a$  and depth  $h$ ) and a dielectric layer unlimited in space (fixed thickness  $\tau$ ). The DTLWA is considered in the radiation mode when the aperture is excited by a slow wave of a dielectric waveguide of the lowest  $E$ -type.

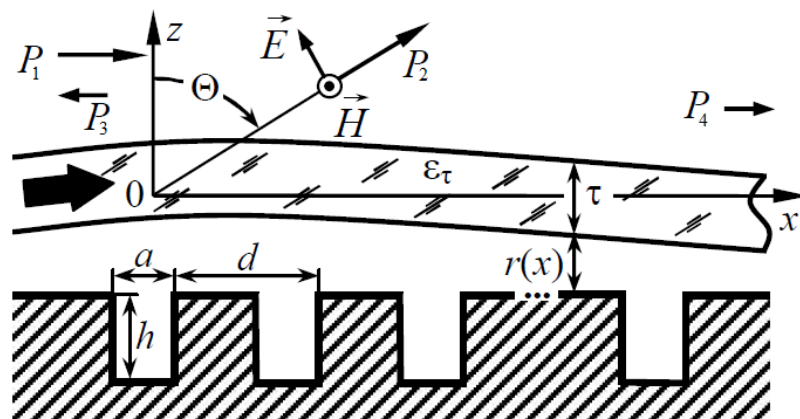


**Figure 1.** Cross-section of the model geometry of the distribution-radiating system of DTLWA

To establish the pattern of change in the impact distance  $r(x)$  (Fig. 1), it is proposed to use a variant of the widespread energy calculation method adapted to the conditions of the problem under consideration - the method of distributed parameters [10, 11]. According to this method, discrete emitters (in the problem under consideration, the grooves of a diffraction grating) generate a discrete amplitude distribution, and the longitudinal intensity of the power take-off is determined by the attenuation of the wave in an open transmission line due to radiation. In this case, one emitter introduces attenuation corresponding to the period of the distribution-radiating system.

Thus, finding the preferred pattern of change in the impact distance  $r(x)$  in DTLWA can be reduced to the task of determining the fraction of power taken by each emitter in accordance with a given amplitude distribution in the aperture. It should be noted that in practice, the distribution of the amplitude distribution of the “cosine on a pedestal” type, which is optimal in terms of the surface utilization factor and the maximum level of side lobes, has become widespread [10]. Then the specified amplitude-phase distribution in the opening can have the form:

$$\dot{v}(k) = \left[ (1 - \Omega) \cos\left(\pi \frac{x_k - 0,5L_A}{L_A}\right) + \Omega \right] \exp(j\beta x_k), \quad (1.a)$$

where  $\Omega$  is the relative field amplitude at the aperture edges,  $L_A$  is the aperture length,  $\beta$  is the free space wavenumber,  $x_k$  is the coordinate of the center of the  $k$ -th groove of the diffraction grating.

### 3. Method for Calculating the Best Regularity of the Longitudinal Variation of the Aiming Distance According to a Given Amplitude Distribution

Let, in order to provide a given amplitude distribution  $v(k)$ , for each  $k$ -th groove of the diffraction grating, the following condition is satisfied [10]:

$$v^2(k) = Fp_k P_1^k = FP_2^k, \tag{1.b}$$

where  $F$  is the normalizing factor,  $p_k$  is the power take-off factor for the  $k$ th groove,  $P_1^k$  is the power of the primary wave supported by a flat dielectric waveguide and exciting the  $k$ -th groove of the diffraction grating.

In (1), the square of the amplitude distribution in the DTLWA opening is presented as a functional dependence on the power take-off coefficients  $p_k$ . Therefore, if the power of the primary excitation wave incident on the  $k$ th groove is  $P_1^k$ , then, in accordance with the approximate model [12-14], the power of the exciting subsequent groove is:

$$P_1^{k+1} = P_1^k - (P_2^k + P_0^k + P_3^k) = P_1^k (1 - p_k - R_k - \Delta_\delta) = P_4^k - P_2^k, \tag{2}$$

where  $P_2^k$  is the power of the wave reflected from the  $k$ -th groove ( $R_k$  is the reflection coefficient),  $P_3^k$  is the power of the losses arising from the interaction of the excitation wave with the  $k$ -th groove.

Note that the value  $\Delta_\delta = \frac{P_3^k}{P_2^k}$ , which determines it, is taken for all grooves to be the same and equal

to the relative power of the loss per unit length in a flat dielectric waveguide. To calculate the specific attenuation, it is reasonable to use the following approximation [15]:

$$\Delta_\delta \approx 27,3\sqrt{\varepsilon_\tau} tg \delta / \lambda, \tag{3.a}$$

where  $\lambda$  is the wavelength,  $\varepsilon_\tau$  and  $tg \delta$  are the relative permittivity and the dielectric loss tangent of the material of the planar dielectric waveguide.

At the same time, some well-known implementations of the energy method for calculating leaky wave antennas for a given amplitude field distribution in the aperture, described, for example, in [10, 16], take into account only attenuation due to radiation and do not take into account power losses in the transmission line. In such cases, it is often assumed that the wave attenuation in a planar dielectric waveguide can be ignored ( $\Delta_\delta = 0$ ) due to the small effect of losses on the DTLWA performance.

At the same time, such an assumption can lead to unacceptable errors in calculations, including the patterns of variation in the impact distance  $r(x)$  in antennas operating in the short-wavelength part of the microwave. Further, we will make the assumption that the considered DTLWA with a comb diffraction grating can be preliminarily optimized according to the criterion of minimum reflection coefficient due to the implementation of the optimal width and (or) depth of the grooves [8, 17]. The latter makes it possible to neglect in equation (2) the power of the wave reflected from the  $k$ th groove (reflection coefficient  $R_k$ ). Then, the power transmission coefficient for the  $k$ -th groove of the diffraction grating can be taken equal to;

$$t_k = \frac{P_1^{k+1}}{P_1^k} = 1 - p_k - \Delta_\delta. \quad (3.b)$$

As a result, for the  $k$ th groove, we obtain the following power balance equation:

$$P_1^k = P_1^{k-1} - p_{k-1} P_1^{k-1} - P_3^{k-1} = P_1^{k-1} (1 - p_{k-1} - \Delta_\delta) = P_1^1 \prod_{m=1}^{k-1} (1 - p_m - \Delta_\delta) = P_1^1 \prod_{m=1}^{k-1} t_m, \quad (4)$$

for a grating consisting of  $N$  grooves,

$$P_1^{N+1} = P_1^1 \prod_{k=1}^N t_k = P_1^1 T_1, \quad (5)$$

where  $T_1$  is the power transmission coefficient of the primary excitation wave to the periphery of the distribution-radiating system of DTLWA.

Let us find the power take-off coefficients  $p_k$  for a given amplitude distribution  $v(k)$ . To do this, from equations (1) and (4) we obtain:

$$\sum_{k=1}^N v^2(k) = F \sum_{k=1}^N p_k P_1^k = F \sum_{k=1}^N (P_1^k - P_1^{k+1}) = F(P_1^1 - P_1^{N+1}) = F(P_1^1 - T_1 P_1^1) = F P_1^1 (1 - T_1). \quad (6.a)$$

Therefore, the normalizing factor  $F$  can be defined as

$$F = \frac{1}{P_1^1 (1 - T_1)} \sum_{k=1}^N v^2(k). \quad (6.b)$$

We substitute equations (4), (6) into (1) and exclude (1)  $P_1^1$ , after which we obtain:

$$p_k = \frac{1 - T_1}{\prod_{m=1}^{k-1} (1 - p_m - \Delta_\delta)} \frac{v^2(k)}{\sum_{k=1}^N v^2(k)}. \quad (7)$$

The power take-off coefficients  $p_k$  are completely determined by the given normalized amplitude distribution of the field in the aperture  $v(k)$ , power transmission coefficient  $T_1$  and per unit attenuation  $\Delta_\delta$  in a flat dielectric waveguide. Note that the maximum achievable value of the selection coefficient for the  $k$ -th groove should not exceed one.

As the initial data for the implementation of the presented technique, in addition to the given amplitude distribution in the opening, the dependence of the power takeoff in DTLWA

$\frac{P_1}{P} = \frac{P_1^1}{P_1^{N+1}} = \frac{1}{T_1}$  on the value of the aiming distance  $r$  is used. Note that this dependence can be

obtained both experimentally [18, 19] and using a reliable mathematical model, for example, described in [20, 21]. Thus, at the initial stage of synthesis of DTLWA using the electrodynamic model of diffraction of a given surface wave of a plane dielectric waveguide on a finite comb grating [22, 23], one should obtain the dependence of the power take-off on the impact distance, taking into account the balance:  $P_2 + P_0 + P = P_1$ . Further, assuming that unit power ( $P_1^1 = 1$ ) is supplied to the

antenna input, the power take-off  $\frac{P_1^k}{P_1^{k+1}}$  is calculated for each  $k$ -th groove of the diffraction grating using equations (4), (6) and (7). Then, according to the known dependence of the power take-off, the required intensity of the take-off for each  $k$ -th groove of the diffraction grating is determined, and from it, in turn, the aiming distance for the  $k$ -th period of the comb is restored. Thus, according to the given amplitude distribution, the transmission coefficient, the relative power loss in a planar dielectric waveguide, the calculated power take-off coefficients, and the established dependence of the power take-off on the impact distance, it is possible to unambiguously determine the pattern of the best longitudinal change in the profile  $r(x)$ .

#### 4. Synthesis of an Antenna with a Longitudinal Variation of the Aiming Distance

Using the method presented below, a structural-parametric synthesis of a DTLWA designed for operation in the frequency band of 9-10 GHz was performed. As a synthesized distribution-radiating system, a covered flat dielectric waveguide, an equidistant comb diffraction grating with 22 grooves of the same width and depth, was taken, optimized at the first stage of synthesis according to the criterion of maximum efficiency (more than 90%) at the center frequency. The distance between adjacent grooves  $d$  (comb pitch) is taken to be commensurate with the wavelength and is  $0,76\lambda$ , which at  $\lambda = 31,6 \text{ mm}$  corresponds to the average frequency of the operating range of 9,5 GHz. The thickness of the planar dielectric waveguide is chosen taking into account the fulfillment of the single-mode waveguide condition:

$$\tau \leq \frac{\lambda}{2\sqrt{\varepsilon_r - 1}}. \quad (8)$$

The relative permittivity  $\varepsilon_r$  of the material of a planar dielectric waveguide was taken equal to 2,55, which corresponds to Preperm 255 polymer. During the synthesis, it was assumed that the value of the air gap  $r$  between the flat dielectric waveguide and the diffraction grating is not less than  $(0,3-0,75) \lambda$  [17, 24, 25]. Since the optimized aperture of the antenna is excited by the  $E$ -wave of a plane dielectric waveguide of the lowest type, so that the radiated wave is vertically polarized, in order to realize the maximum radiative capacity of the grooves of the comb diffraction grating, their width is taken equal to half the period –  $0,5d$ . The groove depth was chosen somewhat less than the resonant depth:  $0,634 \lambda/4$  [26].

For the specified parameters of the radiating aperture, the calculated efficiency at a frequency of 9,5 GHz was 97%, the direction of maximum radiation was  $106^\circ$ . According to the results of the first stage of the structural-parametric synthesis, the design parameters of the DTLWA are determined as follows: period ( $d$ ), length ( $L_A$ ) and width of the diffraction grating ( $W$ ) - 24, 540 and 53 mm, respectively; depth ( $h$ ) and width of grooves ( $a$ ) - 5 and 12 mm; thickness ( $\tau$ ) and initial impact distance of a flat dielectric waveguide ( $r$ ) - 6 and 10 mm. The virtual prototype of the antenna is shown in Fig. 2 in isometric view.

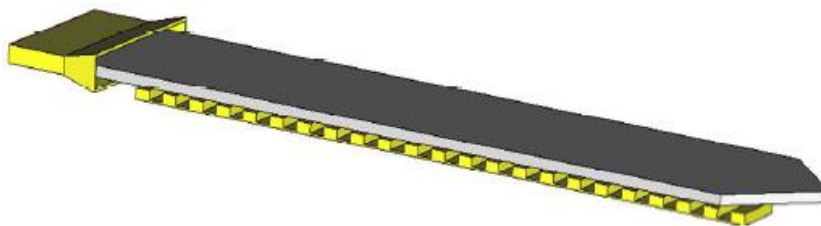


**Figure 2.** Virtual antenna prototype in isometric view

To implement the simulation shown in Fig. 2 of the electrodynamic structure and its subsequent modifications, we used the time domain solver of the CST Studio Suite simulator (with an academic license), based on the Weiland finite integration method [27]. On Fig. 3, a, b shows the radiation patterns of the studied antenna at a frequency of 9,5 GHz, from which, in particular, it follows that the maximum side lobe level is “minus” 7,9 dB, the gain is 20,7 dB. The width of the radiation patterns in the vertical plane is 4,1°, the direction of maximum radiation is 103°. Note that the maximum level of the side lobe was not small enough. The latter can be explained by the decreasing amplitude distribution of the field (Fig. 3, c), which is not optimal both from the standpoint of ensuring a low level of side lobes and a high area utilization factor, and, therefore, it is advisable to further optimize the distribution-radiating system from the position implementation in the aperture of a more suitable amplitude distribution, for example, the “cosine on a pedestal” type. In addition to simulation modeling, the amplitude distribution in the aperture was additionally calculated by two more methods (Fig. 3, c): using the representation of the field by the Kirchhoff formula at fixed points above the aperture (according to [28]) and integrating the spectral density of the field amplitudes in the direction leakage of a surface wave with respect to the spatial frequency (based on the model [29]).

It is also important to note that there are some restrictions on the shape of the amplitude distribution [17, 20]. Thus, the amplitude distribution curve must be a continuous, smooth function and cannot take zero values, including the peripheral points of the radiating aperture. The last limitation is due to the fact that at a zero amplitude value in the aperture, the corresponding power take-off value is 0 dB, which is achieved only at an infinitely large aiming distance. Therefore, such well-known amplitude distributions as “cosine” or “cosine-square” can only be realized with a finite value pedestal, which is typical for openings used in practice [17].

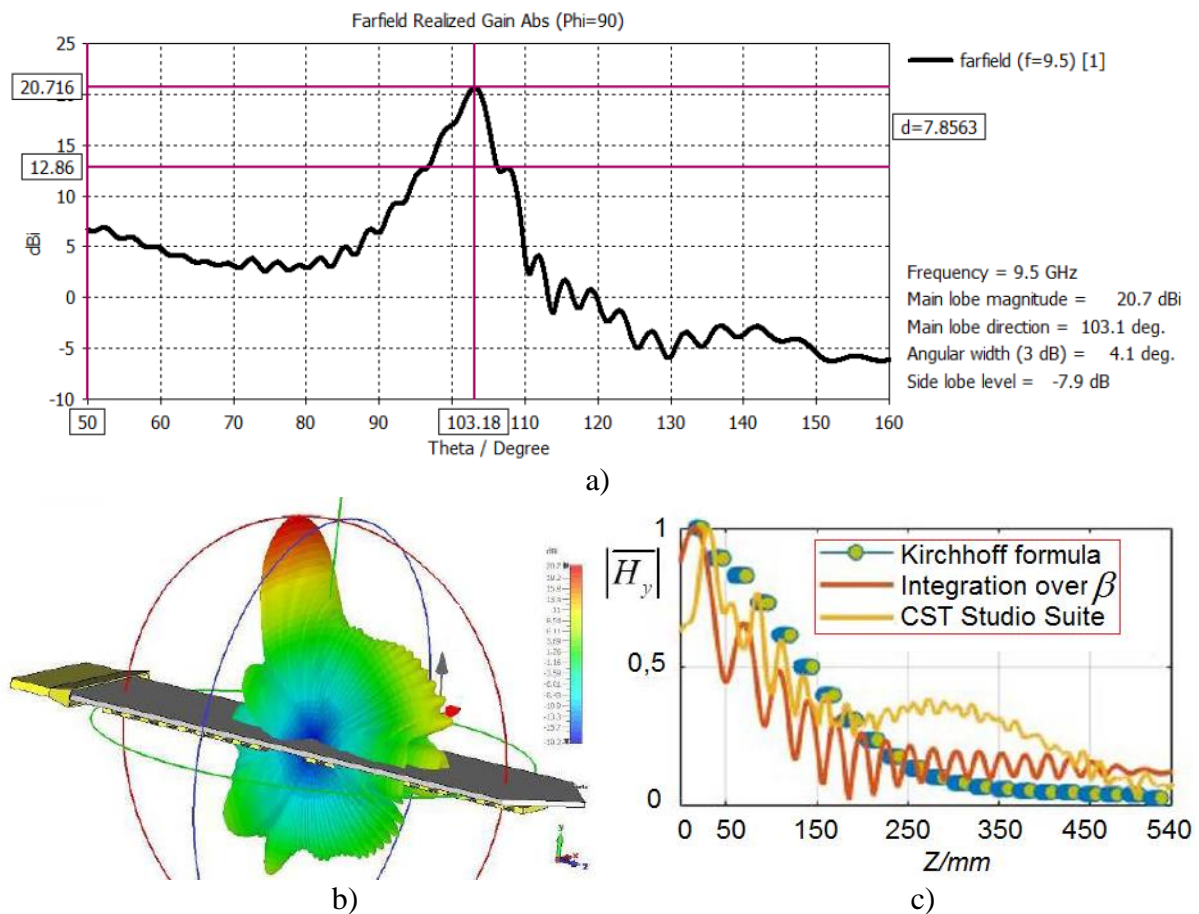


**Figure 3.** Antenna patterns at 9,5 GHz: a) angle versus gain; b) 3D radiation patterns; c) amplitude distribution of the electromagnetic field

The second stage of synthesis consists, in fact, in finding the best pattern for the longitudinal variation of the impact distance  $r(x)$ . Before this, it is advisable to ensure that the field at the periphery of the opening falls to a value of the order of “minus” 30 dB, for which the relative pedestal  $\Omega$  of the given amplitude “cosine” distribution should be taken equal to 0,03. Further, using the electrodynamic model of diffraction of a given surface wave of a plane dielectric waveguide on a finite comb grating [18, 19], it is necessary to obtain a curve of dependence of the power take-off, which provides the radiating aperture, on the value of the impact distance  $r$  (Fig. 4).

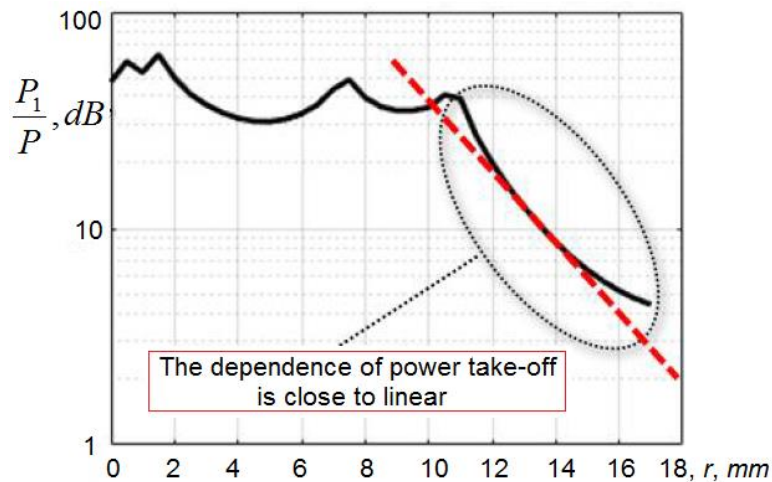


**Figure 4.** Dependences of the power take-off, providing the radiating opening, on the magnitude of the aiming distance

From Fig. 4, in particular, it can be seen that in the initial section of the power take-off curve (when the aiming distance changes from 0 to 10,5 mm), there are pronounced dips. Their presence, as a rule, is due to a significant value of the reflection coefficient of the primary excitation wave. In this case, according to [24], the bulk wave emitted by the antenna is added to the surface wave of a planar dielectric waveguide, which leads to an increase or, on the contrary, a decrease in the field strength that excites the grooves of the comb. Therefore, in order to ensure the optimal regularity in the change in the aiming distance, one should choose the part of the curve that is closest to the linear one. Within such a section of the power take-off curve, a single-valued and monotonic dependence of the power take-off on the impact distance  $r$ , which is typical for a transparent flat dielectric waveguide with a thickness determined by (8), is presumably guaranteed.

The choice of the Preperm 255 compound as a material for a planar dielectric waveguide is due to the fact that it has a high dielectric stability at frequencies up to 120 GHz and relatively low losses ( $tg\delta=0,0005$ ) [25]. In addition, the Preperm 255 dielectric is suitable for implementing 3D printing technology [26], which greatly simplifies the process of manufacturing dielectric waveguides with a complex profile structure. The specific attenuation at a frequency of 9,5 GHz for a dielectric waveguide made of this polymer, calculated using (2), is 0,69 dB/m. The influence exerted by losses on attenuation in a planar dielectric waveguide is illustrated by the longitudinal power take-off curves (Fig. 5, when the opening is excited by a unit power). So, from Fig. 5 it follows that taking into account the specific attenuation in the dielectric waveguide ( $\Delta_s = 0,69\text{ dB/m}$ ) leads to a consistent decrease in the proportion of the incident power (up to a third on the peripheral groove) compared to the case of no losses in the flat dielectric waveguide ( $\Delta_s = 0$ ).

On Fig. 6 shows the calculated dependence of the longitudinal change in the impact distance  $r(x)$ , obtained on the basis of the above method. Aiming distance at this varies from 10,5 to 17 mm.

Despite the fact that the law of change in  $r(x)$  is rather complicated, the curve in Fig. 6 can be divided into three areas:

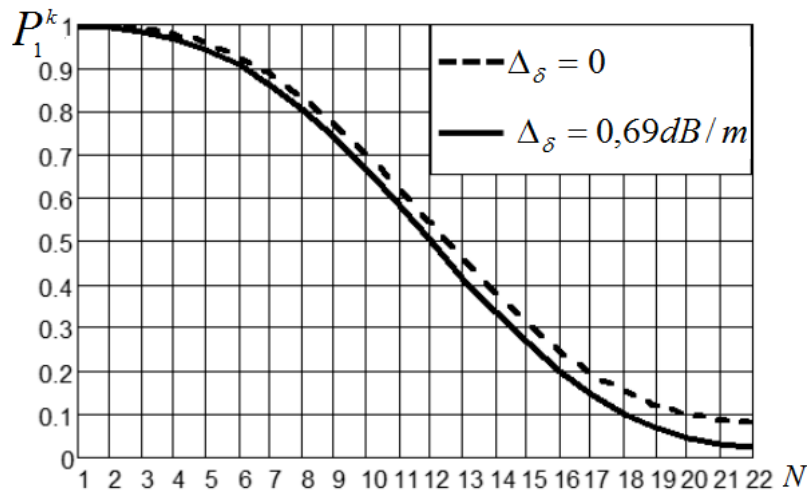


**Figure 5.** Effect of loss on attenuation in a planar dielectric waveguide

- 1) from 0 to 140 mm - the opening area, within which the smallest power take-off for radiation is provided; the aiming distance  $r$  in this area decreases from its maximum value of 17 mm to 16,5 mm;
- 2) from 141 to 450 mm - the area within which the power take-off for radiation increases linearly; aiming distance  $r$  decreases from 16 to 10,5 mm;
- 3) from 451 to 540 mm - the area within which the power take-off decreases, but the aiming distance  $r$  increases from 11 to 11,8 mm.

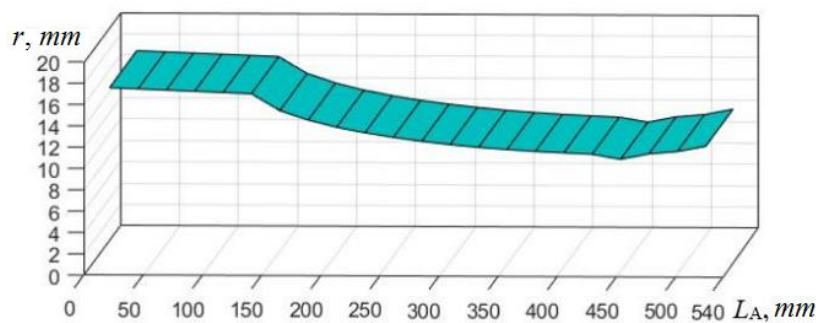


**Figure 6.** Calculated dependence of the longitudinal change of the aiming distance

The obtained pattern of change in the aiming distance can be due to the non-uniformity of the profile of a flat dielectric waveguide. The virtual prototype of the antenna is shown in Fig. 7 in isometric view.

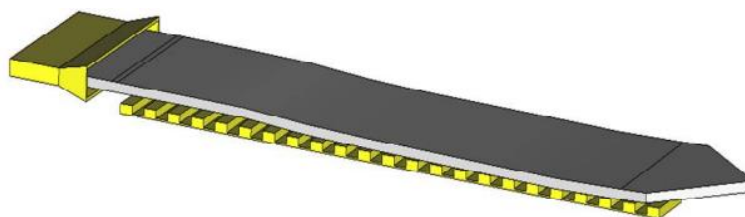


**Figure 7.** Antenna virtual prototype

On Fig. 8, a, b shows the radiation patterns of the antenna with a longitudinal variation of the impact distance, obtained for a frequency of 9,5 GHz. The maximum side lobe level is now minus 13,1 dB, the gain is 22,1 dB. The width of the radiation patterns in the vertical plane is 3,4°, the direction of maximum radiation is 103,3°. The amplitude distribution (Fig. 8, c) has a shape more similar to the “cosine on a pedestal”.

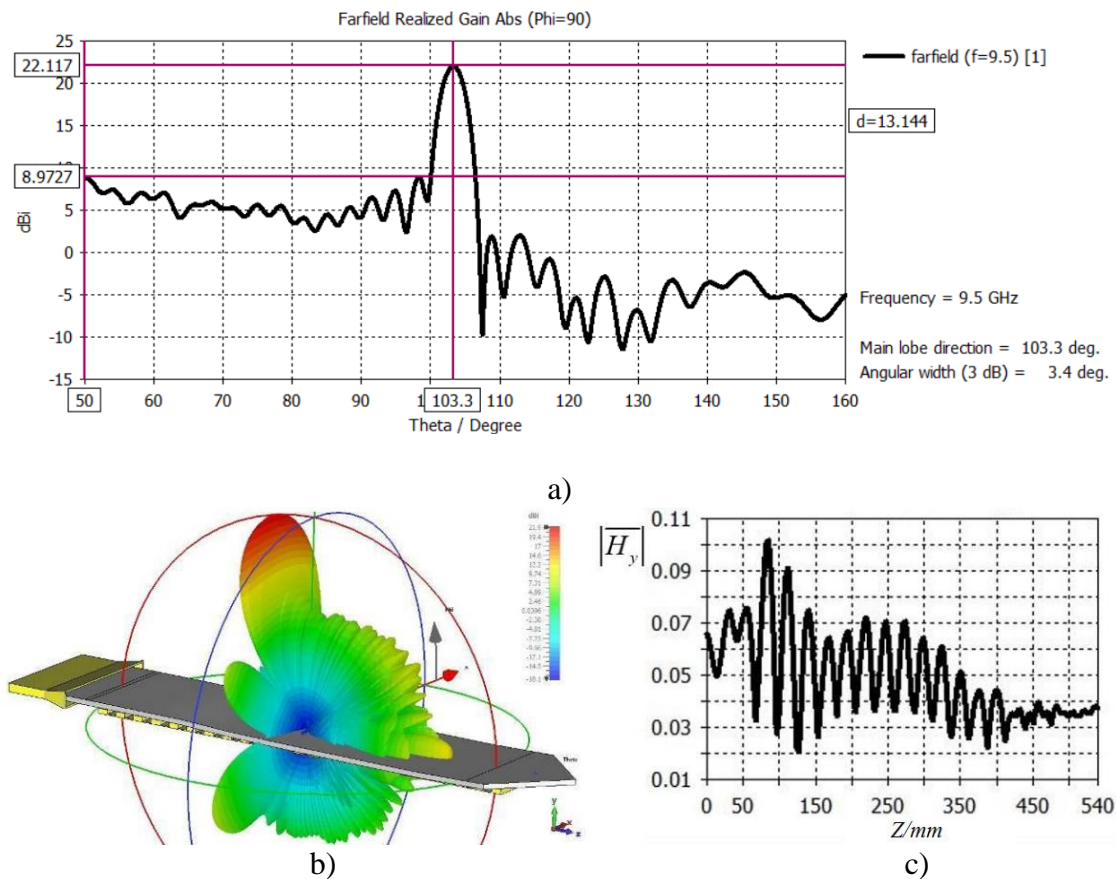


**Figure 8.** Antenna patterns: a) antenna patterns with longitudinal variation of the impact distance obtained for a frequency of 9, 5 GHz; b) 3D model of antenna patterns; c) amplitude distribution of the electromagnetic field

From fig. It follows from Fig. 8 that when changing the aiming distance in accordance with the obtained regularity  $r(x)$  (Fig. 6), it is possible to reduce the level of side lobes by 66% (by 5,2 dB) and at the same time increase the gain by 7% (by 1,4 dB) compared to with the case of a uniform impact distance (Fig. 2). The uneven profile of the flat dielectric waveguide also contributed to improving the focusing of radiation within the main lobe of the radiation patterns without changing the direction of maximum radiation.

### 5. Wedge Gap Between Dielectric Waveguide and Comb Grating

As is known, the implementation of a wedge-shaped gap between a flat dielectric waveguide and a diffraction grating also makes it possible to optimize the amplitude distribution in the antenna aperture to achieve a higher area utilization factor and, accordingly, the overall efficiency of the antenna [8, 9].

On Fig. 9 shows the best performance of the studied antenna, which can be achieved by experimental selection of the wedge-shaped gap. The value of the maximum sidelobe level at a frequency of 9,5 GHz obtained from the simulation results is “minus” 11,7 dB, the gain is 22 dB, the width of the main

lobe of the directivity patterns is  $3,1^\circ$ , the direction of maximum radiation is  $104,3^\circ$ . However, these indicators are still somewhat worse than those of an antenna with an uneven profile of a flat dielectric waveguide (Fig. 8). Differences also manifest themselves in the forms of realized amplitude distributions (Fig. 8, c and Fig. 9, c). At the same time, the exponentially decreasing average value of the amplitude distribution (Fig. 9, c) also does not contribute to achieving the minimum level of lateral radiation.

Based on the simulation results, it has been established that a wedge-shaped gap DTLWA provides acceptable electrical characteristics (close to the characteristics of an antenna with a non-uniform profile for flat dielectric waveguides) only in the lower part of the operating range, at frequencies from 9 to 9,5 GHz. With an increase in the operating frequency, an increase in the maximum level of side lobes is observed, which leads to the appearance of a secondary (side) maximum of the radiation patterns. So, at a frequency of 9,9 GHz for an antenna with a wedge-shaped gap, the maximum side lobe level is “minus” 8,4 dB, and the gain is 22 dB.

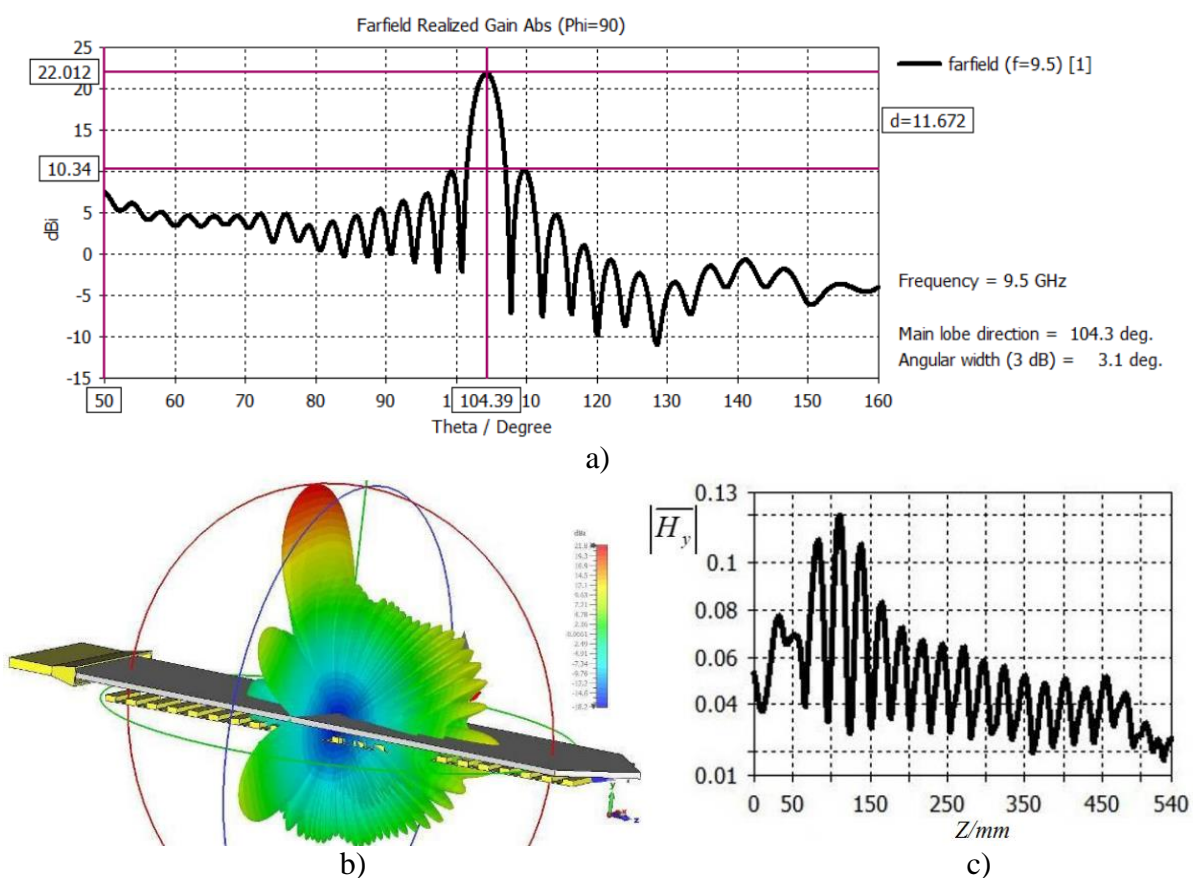


**Figure 9.** The best performance of the studied antenna, which can be achieved by experimental selection of the wedge-shaped gap: a) antenna patterns with longitudinal variation of the impact distance obtained for a frequency of 9, 5 GHz; b) 3D model of antenna patterns; c) amplitude distribution of the electromagnetic field

For comparison, the maximum level of side lobe in an antenna with an uneven profile of a flat dielectric waveguide (Fig. 7) at a frequency of 9,9 GHz is “minus” 12,8 dB, while the gain is 22,5 dB (Fig. 10). The direction of maximum radiation and the width of the radiation patterns at the level of “minus” 3 dB for these antenna options differ slightly (within  $1^\circ$ ). It is also important to note that at the indicated frequency, for an antenna with a uniform profile (Fig. 2), the maximum level of side lobes is only “minus” 6,2 dB, the gain is 21,6 dB. This allows us to make a quite definite conclusion

that the longitudinal variation of the aiming distance, in accordance with the calculated regularity, in some cases, makes it possible to reduce the maximum level of side lobes by more than 100% (by 6,4 dB) compared to the initial value.

The analysis of the obtained results shows that the initial directional properties of the studied antenna can be improved by structural-parametric synthesis using the proposed technique. In this case, the total efficiency of the antenna  $E_{eff}$  with a longitudinal variation of the impact distance  $r(x)$  in accordance with Fig. 6 is from 87 to 90 (Fig. 11). The best overall performance for such an antenna is achieved at operating frequencies from 9,5 to 10 GHz.

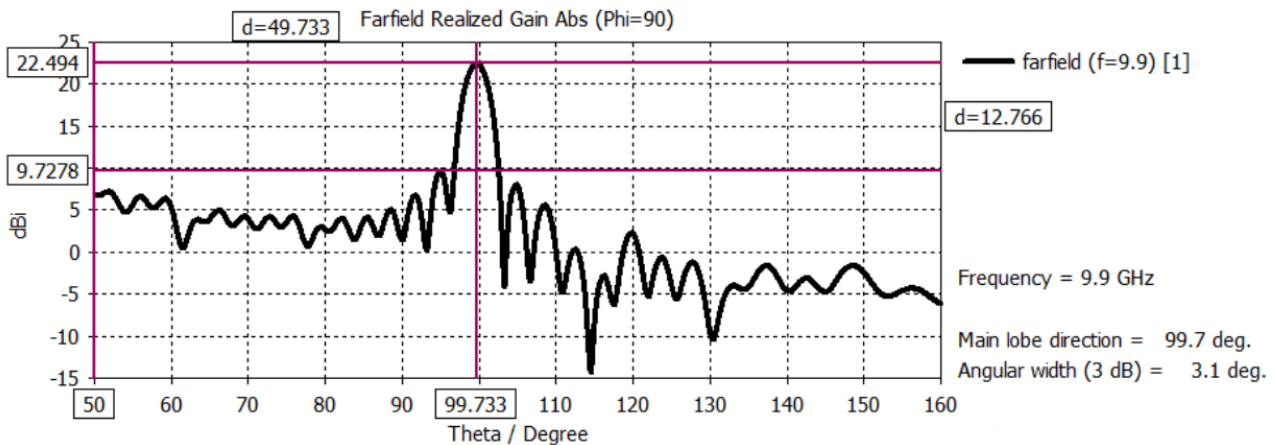


**Figure 10.** Amplitude distribution of the electromagnetic field of the antenna with a gain of 22,5 dB

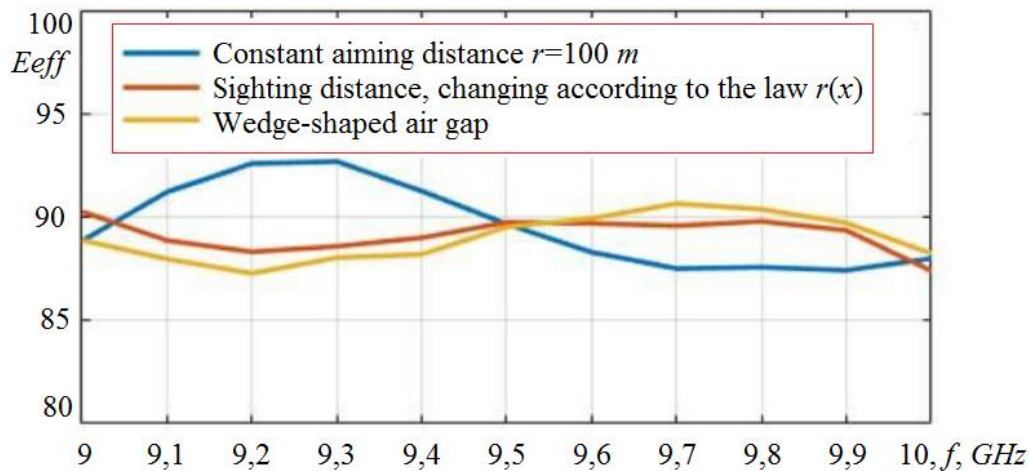


**Figure 11.** Total antenna efficiency  $E_{ff}$  with longitudinal impact distance variation  $r(x)$

When implementing DTLWA based on a distribution-radiating system with a non-uniform profile, high manufacturability is possible. It is guaranteed by widely used modern CAD systems with 3D printing technology. However, excessive variation of the DTLWA profile can lead to noticeable phase distortions in the aperture and deformation of the radiation patterns.

### 6. Conclusions

The paper proposes and tests an effective method for improving the directivity of DTLWA based on the implementation of a longitudinal change in the profile of the distribution-radiating system due to the variation of the aiming distance according to a given amplitude distribution. It has been

established that changing the aiming distance along the aperture according to a theoretically calculated regularity makes it possible to improve the initial directional properties of the antenna: to reduce the maximum level of side lobes, and also to increase the antenna gain.

## Acknowledgments

The author expresses their deep gratitude to the entire editorial board of the journal for their professionalism and excellent work. I especially want to note the very careful and attentive attitude of the reviewers, and their detailed study of the manuscript of the article. Their comments and recommendations are constructive, which allows for improving the quality of the presented research and structuring of the article as much as possible according to the requirements of the journal. The friendly and prompt nature of communication with the editorial board contributes to the rapid resolution of all emerging issues and compliance with the stated deadlines for reviewing and publishing the article.

## Authors' Contributions

All authors contributed equally to this work. Conceptualization, I.I., A.R., M.J., N.S., and R.A.; methodology, I.I., A.R., M.J., N.S., and R.A.; software, I.I., A.R., M.J., N.S., and R.A.; validation, I.I., A.R., M.J., N.S., and R.A.; formal analysis, I.I., A.R., M.J., N.S., and R.A.; investigation, I.I., A.R., M.J., N.S., and R.A.; resources, I.I., A.R., M.J., N.S., and R.A.; data curation, I.I., A.R., M.J., N.S., and R.A.; writing - original draft preparation, I.I., A.R., M.J., N.S., and R.A.; writing - review and editing, I.I., A.R., M.J., N.S., and R.A. All authors have read and agreed to the published version of the manuscript.

## Competing Interests

The authors declare that they have no competing interests.

## References

- [1]. G. Kerim, and B. Suad, "A quantized water cycle optimization algorithm for antenna array synthesis by using digital phase shifters," *International Journal of RF and Microwave Computer-Aided Engineering*, vol. 25, no. 1, pp. 21-29, 2015.
- [2]. H. I. Taisir, and M. H. Zoubir, "Array Pattern Synthesis Using Digital Phase Control by Quantized Particle Swarm Optimization," *IEEE Transactions on Antennas and Propagation*, vol. 58, no. 6, pp. 2142-2145, 2010.
- [3]. P. David, O. Tamas, C. D. G. Deubauh, and K. N. Hamid, "Performance Comparison of Quantized Control Synthesis Methods of Antenna Arrays," *Electronics*, vol. 1, no. 7, pp. 994-102, 2022.
- [4]. S.-T. Sheu, J.-S. Wu, C.-H. Huang, Y.-C. Cheng, and L. Chen, "DDAS: Distance and Direction Awareness System for Intelligent Vehicles," *Journal of Information Science and Engineering*, vol. 23, pp. 709-722, 2007.
- [5]. S. Liang, T. Feng, and G. Sun, "Sidelobe-level suppression for linear and circular antenna arrays via the cuckoo search-chicken swarm optimisation algorithm," *IET Microw. Antennas Propag.*, vol. 11, pp. 209-218, 2017.
- [6]. H. Singh, B. S. Sohi, and A. Gupta, "Designing and performance evaluation of metamaterial inspired antenna for 4G and 5G applications," *Int. J. Electron.*, vol. 108, pp. 1035-1057, 2021.
- [7]. H. Singh, N. Mittal, U. Singh, and R. Salgotra, "Synthesis of non-uniform circular antenna array for low side lobe level and high directivity using self-adaptive Cuckoo search algorithm," *Arab. J. Sci. Eng.*, vol. 47, pp. 3105-3118, 2022.
- [8]. G. Yang, Y. Zhang, and S. Zhang, "Wide-band and wide-angle scanning phased array antenna

- for mobile communication system,” *IEEE Open J. Antennas Propag.*, vol. 2, pp. 203-212, 2021.
- [9]. R. Q. Wang, and Y. C. Jiao, “Synthesis of wideband rotationally symmetric sparse circular arrays with multiple constraints,” *IEEE Antennas Wirel. Propag. Lett.*, vol. 18, pp. 821-825, 2019.
- [10]. L. Hui, C. Yikai, and J. Ulrich, “Synthesis, Control, and Excitation of Characteristic Modes for Platform-Integrated Antenna Designs: A design philosophy,” *IEEE Antennas and Propagation Magazine*, vol. 64, no. 2, pp. 41-48, 2022.
- [11]. R. Castillo, R. Ma, and N. Behdad, “Platform-based electrically-small HF antenna with switchable directional radiation patterns,” *IEEE Trans. Antennas Propag.*, vol. 69, no. 8, pp. 4370-4379, 2021.
- [12]. Y. Liu, J. Zhang, A. Ren, H. Wang, and C. Sim, “TCM-based heptaband antenna with small clearance for metal-rimmed mobile phone applications,” *IEEE Antennas and Wireless Propag. Lett.*, vol. 18, no. 4, pp. 717-721, 2019.
- [13]. I. J. Islamov, E. G. Ismibayli, Y. G. Gaziyev, S. R. Ahmadova, and R. S. Abdullayev, “Modeling of the Electromagnetic Field of a Rectangular Waveguide with Side Holes,” *Progress in Electromagnetics Research*, vol. 81, pp. 127-132, 2019.
- [14]. I. J. Islamov, N. M. Shukurov, R. S. Abdullayev, K. K. Hashimov, and A. I. Khalilov, “Diffraction of Electromagnetic Waves of Rectangular Waveguides with a Longitudinal,” *Application in Information and Telecommunication Systems*, pp. 35-46, 2020.
- [15]. A. I. Khalilov, I. J. Islamov, E. Z. Hunbataliyev, N. M. Shukurov, and R. S. Abdullayev, “Modeling Microwave Signals Transmitted Through a Rectangular Waveguide,” *Application in Information and Telecommunication Systems*, pp. 56-67, 2020.
- [16]. I. J. Islamov, and E. G. Ismibayli, “Experimental Study of Characteristics of Microwave Devices Transition from Rectangular Waveguide to the Megaphone,” *IFAC-PapersOnLine*, vol. 51, no. 30, pp. 477-479, 2018.
- [17]. E. G. Ismibayli, and I. J. Islamov, “New Approach to Definition of Potential of the Electric Field Created by Set Distribution in Space of Electric Charges,” *IFAC-PapersOnLine*, vol. 51, no. 30, pp. 410-414, 2018.
- [18]. I. J. Islamov, E. G. Ismibayli, M. H. Hasanov, Y. G. Gaziyev, S. R. Ahmadova, and R. S. Abdullayev, “Calculation of the Electromagnetic Field of a Rectangular Waveguide with Chiral Medium,” *Progress in Electromagnetics Research*, vol. 84, pp. 97-114, 2019.
- [19]. I. J. Islamov, E. Z. Hunbataliyev, and A. E. Zulfugarli, “Numerical Simulation of Characteristics of Propagation of Symmetric Waves in Microwave Circular Shielded Waveguide with a Radially Inhomogeneous Dielectric Filling,” *International Journal of Microwave and Wireless Technologies*, vol. 9, pp. 761-767, 2021.
- [20]. I. J. Islamov, M. H. Hasanov, and M. H. Abbasov, “Simulation of Electrodynamics Processes in a Cylindrical-Rectangular Microwave Waveguide Systems Transmitting Information,” *Theory and Application of Soft Computing, Computing with Words, Perception and Artificial Intelligence*, pp. 246-253, 2021.
- [21]. A. G. Charles, and Y. Guo, “A General Approach for Synthesizing Multibeam Antenna Arrays Employing Generalized Joined Coupler Matrix,” *IEEE Transactions on Antennas and Propagation*, vol. 256, pp. 1-10, 2022.
- [22]. A. K. Amin, “A Proposed Method for Synthesizing the Radiation Pattern of Linear Antenna Arrays,” *Journal of Communications*, vol. 17, no. 7, pp. 1-6, 2022.
- [23]. A. Zeeshan, U. A. J. Zain, B. Shu-Di, and C. Meng, “Comments on Frequency Diverse Array Beampattern Synthesis with Taylor Windowed Frequency Offsets,” *IEEE Antennas and Wireless Propagation Letters*, vol. 21, no. 8, pp. 1713-1714, 2022.
- [24]. Z. Wang, Y. Song, T. Mu, and Z. Ahmad, “A short-range range-angle dependent beampattern synthesis by frequency diverse array,” *IEEE Access*, vol. 6, pp. 22664-22669, 2018.
- [25]. X. Shao, T. Hu, Z. Xiao, and J. Zhang, “Frequency 1+ synthesis with modified sinusoidal frequency offset,” *IEEE Antennas Wireless Propag. Lett.*, vol. 20, no. 9, pp. 1784-1788, 2021.
- [26]. R. Quanxin, Q. Bingyi, C. Xiaoming, H. Xiaoyu, L. Qinlong, and Z. Jiaying, “Linear Antenna

- Array with Large Element Spacing for Wide-Angle Beam Scanning with Suppressed Grating Lobes,” *IEEE Antennas and Wireless Propagation Letters*, vol. 21, no. 6, pp. 1258-1262, 2022.
- [27]. G. Yang, Y. Zhang, and S. Zhang, “Wide-band and wide-angle scanning phased array antenna for mobile communication system,” *IEEE Open J. Antennas Propag.*, vol. 2, pp. 203-212, 2021.
- [28]. Y.-F. Cheng, X. Ding, W. Shao, M.-X. Yu, and B.-Z. Wang, “A novel wide-angle scanning phased array based on dual-mode pattern reconfigurable elements”, *IEEE Antennas Wireless Propag. Lett.*, vol. 16, pp. 396-399, 2017.
- [29]. J. Zhang, X. Cui, H. Xu, S. Zhao, and M. Lu, “Efficient Signal Separation Method Based on Antenna Arrays for GNSS Meaconing,” *Tsinghua Science and Technology*, vol. 24, no. 2, pp. 216-225, 2019.